



**HAL**  
open science

## Modeling of hysteresis by means of a directional approach. Constitutive Models

Thierry Rey, Grégory Chagnon, Denis Favier, Jean-Benoit Le Cam

### ► To cite this version:

Thierry Rey, Grégory Chagnon, Denis Favier, Jean-Benoit Le Cam. Modeling of hysteresis by means of a directional approach. Constitutive Models. 8th European Conference on Constitutive Models for Rubbers, Jun 2013, San Sabastian, Spain. pp.107-110. hal-00936538

**HAL Id: hal-00936538**

**<https://hal.science/hal-00936538>**

Submitted on 26 Jan 2014

**HAL** is a multi-disciplinary open access archive for the deposit and dissemination of scientific research documents, whether they are published or not. The documents may come from teaching and research institutions in France or abroad, or from public or private research centers.

L'archive ouverte pluridisciplinaire **HAL**, est destinée au dépôt et à la diffusion de documents scientifiques de niveau recherche, publiés ou non, émanant des établissements d'enseignement et de recherche français ou étrangers, des laboratoires publics ou privés.



Distributed under a Creative Commons Attribution 4.0 International License

# Modeling of hysteresis by means of a directional approach

T. Rey<sup>(1)</sup> & G. Chagnon<sup>(1)</sup> & D. Favier<sup>(1)</sup> & J.-B. Le Cam<sup>(2)</sup>

(1) *Université de Grenoble/CNRS, Laboratoire 3SR, domaine universitaire, 38041 Grenoble cedex 9, France.*

(2) *Université de Rennes 1, L.A.R.M.A.U.R. - CNRS 6274, Campus de Beaulieu, Bât. 10B, 35042 Rennes Cedex, France.*

**ABSTRACT:** This paper focuses on the mechanical hysteresis in elastomers, i.e. the difference between loading and unloading paths. This property can be time-dependent as well as time-independent, depending on the physical phenomena that come into play. Similarly, mechanical hysteresis can be affected or not by material anisotropy. In this context, the present study is devoted to the modeling of time-independent hysteresis, in the framework of material anisotropy, accommodated to the Mullins effect. For this purpose, directional model is used to predict the tridimensional response of such materials. The proposed model is based on the stress decomposition into two parts. The first one represents the hyperelasticity of the macromolecular network, whereas the second part represents the friction in the network, i.e. the hysteretic part. Experiments were carried with filled silicone rubber and results show that the model predictions and experimental curves fit well.

## 1 INTRODUCTION

The characterization and modeling of rubber-like materials behavior have been widely addressed in last decades due to the increasing number of industrial applications. In order to improve the physical properties of the material, silicone rubbers are classically filled by mineral fillers, implying an increase of stiffness but also the appearance of some unconventional effects. Among these phenomena, one can cite the stress softening, which principally occurs between first and second loads, often called the Mullins effect (Mullins, 1948), the relaxation and the hysteretic behavior (unload different from load), non-exhaustively.

Moreover, the load and unload responses of a rubber-like material differ during cyclic tests and form a mechanical hysteresis. This phenomenon depends on the strain rate (Amin *et al.*, 2006), the crosslinks density (Bergström and Boyce, 1998) and the temperature (Rey *et al.*, 2013b).

Several micro-motivated (Bergström and Boyce, 1998; Miehe and Göktepe, 2005; D'Ambrosio *et al.*, 2008; Lorenz and Klüppel, 2012) and phenomenological (Dorfmann and Ogden, 2003) approaches of the mechanical hysteresis were published in the literature.

Despite the large number of papers focusing on the viscoelastic behavior of the material, very few studied the rate-independent hysteresis (Kaliske and Rothert, 1998; Vandenbroucke *et al.*, 2010). In order to distinguish stress-softening and hysteresis, very few au-

thors remove the Mullins effect from the material by carrying out several previous mechanical cycles (Lion, 1996; Bergström and Boyce, 1998).

This paper focuses on the quasi-static modeling (*i.e.* the rate independent behavior) of this hysteresis phenomenon after stress softening. The aim of this work is to propose a directional method able to predict the difference between load and unload curves, usable with existing models, and easily extendable to anisotropy. The proposed theory to model hysteresis is introduced in part 2. In part 3, the experimental data are compared with simulations and these results are discussed. Finally, some concluding remarks close the paper.

## 2 THEORY

### 2.1 *Material behavior*

Classically, models are based on a decomposition of the material behavior into several contributions related to different physical phenomena. As an example, a first hyperelastic part can be coupled to a viscous part, a damage part or both of them. As the viscosity is not taken into account in this paper, the model used contains only a hyperelastic part, represented by a non linear spring, and a hysteretic part, represented by an infinity of spring-friction slider associations. Even if this kind of representation is used for the elastomers, it comes from the modeling of other materials behav-

ior, as that of for metallic alloys (Guélin, 1980; Favier and Guélin, 1985).

The mechanical response of the material is, in this paper, obtained by adding the two previous parts, as previously done in Favier (1988); Favier *et al.* (1992) for shape memory alloys and magnetisation phenomena. The total response, with the incompressibility hypothesis, is defined as:

$$\boldsymbol{\sigma} = \boldsymbol{\sigma}_{rev} + \boldsymbol{\sigma}_{hyst} - p\mathbf{I} \quad (1)$$

where  $p$  is the hydrostatic pressure.

## 2.2 Hyperelastic part

Any hyperelastic potential can be used. In this paper, the model proposed by Biderman (1958) is chosen:

$$W_{rev} = c_{10}(I_1 - 3) + c_{20}(I_1 - 3)^2 + c_{30}(I_1 - 3)^3 + c_{01}(I_2 - 3) \quad (2)$$

where  $c_{10}$ ,  $c_{20}$ ,  $c_{30}$  and  $c_{01}$  are material parameters,  $I_1$  and  $I_2$  are respectively the first and second invariants of the right Cauchy-Green tensor defined as  $I_1 = \text{tr}(\mathbf{C})$  and  $I_2 = \frac{1}{2}(\text{tr}(\mathbf{C})^2 - \text{tr}(\mathbf{C}^2))$ .

## 2.3 Hysteresis part

### 2.3.1 General form

A model with an infinity of directions in the space is used. In the case of an initially isotropic material, chains are assumed to be equidistributed in space. This approach was previously used in the literature (Wu and Van der Giessen, 1993). However, to avoid integration problems, a discrete number of directions is used. Here, the 42 directions representation of Bažant and Oh (1986), even if other special repartitions can be chosen. This representation was already used to model rubber-like materials, particularly Mullins effect, see for example Itskov *et al.* (2006), Diani *et al.* (2006) and Rebouah *et al.* (2013). Initial directional vectors  $\mathbf{a}_0^{(i)}$  are defined, and initial direction tensors  $\mathbf{A}_0^{(i)}$ , current direction vectors  $\mathbf{a}^{(i)}$  and tensors  $\mathbf{A}^{(i)}$  are respectively calculated by:

$$\begin{aligned} \mathbf{A}_0^{(i)} &= \mathbf{a}_0^{(i)} \otimes \mathbf{a}_0^{(i)} \\ \mathbf{a}^{(i)} &= \mathbf{F}\mathbf{a}_0^{(i)} \\ \mathbf{A}^{(i)} &= \mathbf{a}^{(i)} \otimes \mathbf{a}^{(i)} \end{aligned} \quad (3)$$

where  $\mathbf{F}$  is the deformation gradient.

By means of the spatial repartition, only monodimensional constitutive equations are needed to represent a tridimensional behavior. No tridimensional generalization of monodimensional constitutive equations (Favier *et al.*, 1992) are needed as in Laurent *et al.* (2008) and Vandenbroucke *et al.* (2010).

In each direction ( $i$ ) the considered constitutive equation during the first load is expressed as:

$$\sigma^{(i)} = S_0 \tanh \frac{E \ln I_4^{(i)}}{2\sigma_0} \quad (4)$$

where  $\sigma^{(i)}$  is the Cauchy stress in the considered direction,  $E$  is equivalent to an initial slope,  $\sigma_0$  is the maximum reachable Cauchy stress by the hysteresis part on each direction  $a_0^{(i)}$ , and  $I_4^{(i)}$  is the fourth invariant of the right Cauchy-Green tensor ( $\mathbf{C} = \mathbf{F}^T\mathbf{F}$ ) defined as  $I_4^{(i)} = \text{tr}(\mathbf{C}\mathbf{A}_0^{(i)})$ , where  $\text{tr}$  means the trace. The chains are assumed to bring a contribution to the material behavior only in the case of a tension loading. Thus, they have no significant contribution in compression. The stress tensor is finally obtained by summing the contributions of each direction:

$$\boldsymbol{\sigma}_{hyst} = \sum_i^{42} \omega_i \sigma^{(i)} \left( \mathbf{A}^{(i)} - \frac{I_4^{(i)}}{3} \mathbf{I} \right) \quad (5)$$

where  $\omega_i$  are the weight corresponding to the considered direction, defined by Bažant and Oh (1986), and  $\mathbf{I}$  the identity tensor.

### 2.3.2 Inversion point

Inversion points are introduced to create the difference between loads and unloads (Guélin, 1980; Wack *et al.*, 1983). At the end of a load, the constitutive equation in a direction ( $i$ ) during unloading is expressed as:

$$\sigma^{(i)} = \sigma_{inv}^{(i)} - \sigma_0 \tanh \frac{E(\ln I_{4inv}^{(i)} - \ln I_4^{(i)})}{2\sigma_0} \quad (6)$$

where  $\sigma_{inv}^{(i)}$  and  $\ln I_{4inv}^{(i)}$  are respectively the stress and strain of the last inversion point. It is to note that this equation is the same as Eq. (4) except the change in the origin function. The readers can refer to Rey *et al.* (2013a) for further informations.

## 3 EXPERIMENTAL VALIDATION

### 3.1 Material

The rubber-like material used is a filled silicone (Bluestar RTV 3428). The mechanical properties of this material were investigated by Machado *et al.* (2010, 2012) and Rey *et al.* (2013b).

### 3.2 Experimental devices and specimen preparations

Different uniaxial tensile tests are carried out in order to validate the model. These tests are performed by means of the Gabo Eplexor 500N, whose load cell capacity is 25N. The length, width and thickness of the

uniaxial tensile tests specimens are 12, 2 and 2 mm respectively.

Preconditioning tests are carried out on the specimens to remove the Mullins effect. This enables us to ensure the repeatability of the tests (Lion, 1996; Bergström and Boyce, 1998; Dorfmann and Ogden, 2004). This preconditioning procedure consists in performing 5 cycles of load-unload at a maximum stretch of 3, with an strain rate equal to  $1.67s^{-1}$ .

First investigations carried out by Rey *et al.* (2013a) demonstrate that strain rate inferior to  $1.67s^{-1}$  does not influence the mechanical behavior.

### 3.3 Loading conditions

Different uniaxial tensile tests are carried out. A first cyclic test is performed from 1.25 to 2.5 stretch level, with an increase of 0.25 between each cycle.

Two additional uniaxial tensile tests are performed to characterize the hysteresis phenomenon. The first test (called nc1 in the following) is a load-unload cycle with two hysteresis loops during the load and the unload. The second (nc2) is a load-unload cycle with a hysteresis subloop inside a first loop during the load.

## 4 MODEL VALIDATION

The constitutive parameters are fitted from experimental data obtained during the first test. They are reported in table 1.

$c_{10}(MPa)$	$c_{20}(MPa)$	$c_{30}(MPa)$
0.095	-0.0015	0.00059
$c_{01}(MPa)$	$E(MPa)$	$S_0(MPa)$
0.03	0.9409	0.06

Table 1: Values of the material parameters fitted on experimental data.

The simulation of the first uniaxial tensile test with increasing cycles from 1.25 to 2.5 stretch level is shown in figure 1, where the nominal stress (or Piola-Kirchhoff 1 stress, *i.e.* the current force divided by the initial section) versus the stretch  $\lambda$  (*i.e.* the ratio between current and initial length) is plotted. It can be seen in this figure that the silicone behavior is well predicted by the model for this experiment as the two curves are nearly superposed. The results of the simulation of 'nc1' is presented in figure 2. In this case, the model gives a reasonable prediction of the stress response of the behavior. Figure 3 shows the results of the simulation of the test 'nc2'. The curves are nearly counfounded, meaning that the model gives good predictions of the material behavior in this case.

## 5 CONCLUSION

A directional elasto-hysteresis model for rubberlike materials was developed in this study. Different uniaxial tests were carried out with hysteresis loops. The

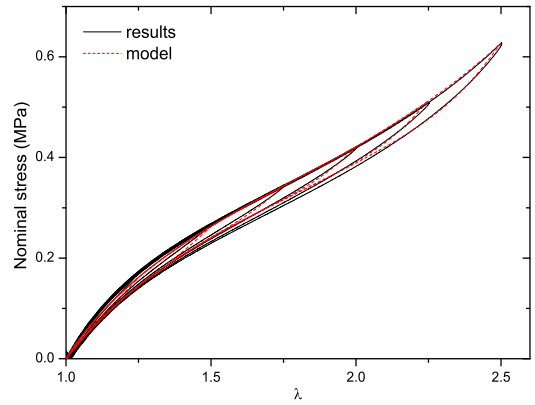


Figure 1: Simulation of a uniaxial tensile test with increasing cycle.

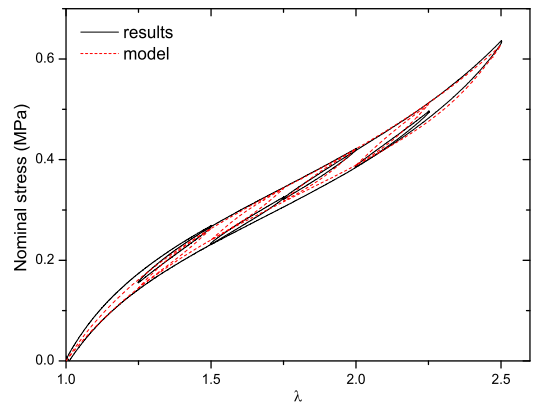


Figure 2: Simulation of a uniaxial tensile test with four hysteresis loops (nc1 test).

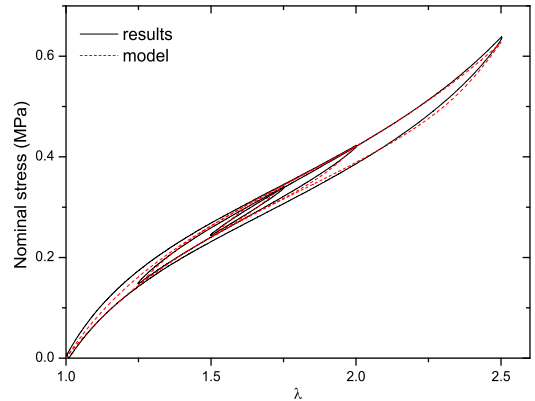


Figure 3: Simulation of a uniaxial tensile test with a hysteresis loop inside another one (nc2 test).

proposed model predicts well the material behavior during these different tests.

Further investigations, like other tests and numerical implementation, are carried out by the authors in Rey *et al.* (2013a).

## 6 ACKNOWLEDGEMENTS

This work is supported by the French National Research Agency Program n2010BLAN90201 ANiM (Architected NiTi Materials).

## REFERENCES

- Amin, A. F. M. S., Lion, A., Sekita, S., and Okui, Y. (2006). Nonlinear dependence of viscosity in modeling the rate-dependent response of natural and high damping rubbers in compression and shear: experimental identification and numerical verification. *Int. J. Plast.*, **22**, 1610–1657.
- Bažant, P. and Oh, B. (1986). Efficient numerical integration on the surface of a sphere. *ZAMM-Journal of Applied Mathematics and Mechanics/Zeitschrift für Angewandte Mathematik und Mechanik*, **66**(1), 37–49.
- Bergström, J. and Boyce, M. (1998). Constitutive modeling of the large strain time-dependent behavior of elastomers. *J. Mech. Phys. Solids*, **46**(5), 931–954.
- Biderman, V. L. (1958). Calculations of rubber parts (in russian). *Rascheti na Prochnost*, page 40.
- D'Ambrosio, P., De Tommasi, D., Ferri, D., and Puglisi, G. (2008). A phenomenological model for healing and hysteresis in rubber-like materials. *Int. J. Eng. Sci.*, **46**, 293–305.
- Diani, J., Brieu, M., and Vacherand, J. (2006). A damage directional constitutive model for Mullins effect with permanent set and induced anisotropy. *Eur. J. of Mech.-A/Solids*, **25**(3), 483–496.
- Dorfmann, A. and Ogden, R. (2003). A pseudo-elastic model for loading, partial unloading and reloading of particle-reinforced rubber. *Int. J. Solids Struct.*, **40**(11), 2699–2714.
- Dorfmann, A. and Ogden, R. (2004). A constitutive model for the Mullins effect with permanent set in particle-reinforced rubber. *Int. J. Solids Struct.*, **41**(7), 1855–1878.
- Favier, D. (1988). *Contribution à l'étude théorique de l'élastohystérésis à température variable, application aux propriétés de mémoire de forme*. Habilitation thesis, University of Grenoble.
- Favier, D. and Guélin, P. (1985). A discrete memory constitutive scheme for mild steel type material theory and experiment. *Arch. Mech.*, **37**, 201–19.
- Favier, D., Guélin, P., and Cammarano, R. (1992). Application of a phenomenological elastohysteretic theory to the modeling of magnetization. In *Seventh International Symposium on Magnetic Anisotropy and Coercivity in Rare-Earth Transition Metal Alloys*.
- Guélin (1980). Remarque sur l'hystérésis mécanique: les bases dun schéma thermo-mécanique à structure héréditaire. *Journal de mécanique*, **19**, 217–247.
- Itskov, M., Haberstroh, E., Ehret, A. E., and Vohringer, M. C. (2006). Experimental observation of the deformation induced anisotropy of the Mullins effect in rubber. *KGK-Kautschuk Gummi Kunststoffe*, **59**(3), 93–96.
- Kaliske, M. and Rothert, H. (1998). Constitutive approach to rate independent properties of filled elastomers. *Int. J. Solids Struct.*, **35**(17), 2057–2071.
- Laurent, H., Vandenbroucke, A., Couedo, S., and Rio, G. (2008). An hyper-visco-hysteretic model for elastomeric behaviour under low and high temperatures: Experimental and numerical investigations. In *Constitutive models for rubber V*, pages 47–52.
- Lion, A. (1996). A constitutive model for carbon black filled rubber: experimental investigations and mathematical representation. *Continuum Mech. Therm.*, **8**(3), 153–169.
- Lorenz, H. and Klüppel, M. (2012). Microstructure-based modelling of arbitrary deformation histories of filler-reinforced elastomers. *J. Mech. Phys. Solids*, **60**, 1842–1861.
- Machado, G., Chagnon, G., and Favier, D. (2010). Analysis of the isotropic models of the Mullins effect based on filled silicone rubber experimental results. *Mech. Mater.*, **42**(9), 841–851.
- Machado, G., Chagnon, G., and Favier, D. (2012). Induced anisotropy by the Mullins effect in filled silicone rubber. *Mech. Mater.*, **50**, 70–80.
- Miehe, C. and Göktepe, S. (2005). A micro-macro approach to rubber-like materials. part ii: The microsphere model of finite rubber viscoelasticity. *J. Mech. Phys. Solids*, **53**(10), 2231–2258.
- Mullins, L. (1948). Effect of stretching on the properties of rubber. *Rubb. Chem. Technol.*, **21**, 281.
- Rebouah, M., Machado, G., Chagnon, G., and Favier, D. (2013). Anisotropic modeling of the Mullins effect based on an invariant formulation. *Mech. Res. Commun.*, **49**, 36–43.
- Rey, T., Chagnon, G., Favier, D., and Le Cam, J.-B. (2013a). Directional elasto-hysteresis mechanical model for rubberlike materials. *Int. J. Solids Struct.*, page In prep.
- Rey, T., Chagnon, G., Le Cam, J.-B., and Favier, D. (2013b). Influence of the temperature on the mechanical behavior of unfilled and filled silicone rubbers. *Polym. Test.*, **32**, 492–501.
- Vandenbroucke, A., Laurent, H., Aït Hocine, N., and Rio, G. (2010). A hyperelasto-visco-hysteresis model for an elastomeric behaviour: Experimental and numerical investigations. *Comp. Mater. Sci.*, **48**(3), 495–503.

- Wack, B., Terriez, J.-M., and Guélin, P. (1983). A hereditary type, discrete memory, constitutive equation with applications to simple geometries. *Arch. Mech.*, **50**, 9–37.
- Wu, P. and Van der Giessen, E. (1993). On improved network models for rubber elasticity and their applications to orientation hardening in glassy polymers. *J. Mech. Phys. Solids*, **41**(3), 427–456.